Orientation of Spindle Axis and Distribution of Plasma Membrane Proteins during Cell Division in Polarized MDCKII Cells

Sigrid Reinsch and Eric Karsenti

European Molecular Biology Laboratory, D69012 Heidelberg, Germany

Abstract. MDCKII cells differentiate into a simple columnar epithelium when grown on a permeable support; the monolayer is polarized for transport and secretion. Individual cells within the monolayer continue to divide at a low rate without disturbing the function of the epithelium as a barrier to solutes. This presents an interesting model for the study of mitosis in a differentiated epithelium which we have investigated by confocal immunofluorescence microscopy. We monitored the distribution of microtubules, centrioles, nucleus, tight junctions, and plasma membrane proteins that are specifically targeted to the apical and basolateral domains. The stable interphase microtubule cytoskeleton was rapidly disassembled at prophase onset and reassembled at cytokinesis. As the interphase microtubules disassembled at prophase, the centrioles moved from their interphase position at the apical membrane to the nucleus and acquired the ability to organize microtubule asters. Orientation of the spindle parallel to the plane of the monolayer occurred between late prophase and metaphase and persisted through cytokinesis. The cleavage furrow formed asymmetrically perpendicular to the plane of the monolayer initiating at the basolateral side and proceeding to the apical domain. The interphase microtubule network reformed after the centrioles migrated from the spindle poles to resume their interphase apical position. Tight junctions (ZO-1), which separate the apical from the basolateral domains, remained assembled throughout all phases of mitosis. E-cadherin and a 58-kD antigen maintained their basolateral plasma membrane distributions, and a 114-kD antigen remained polarized to the apical domain. These proteins were useful for monitoring the changes in shape of the mitotic cells relative to neighboring cells, especially during telophase when the cell shape changes dramatically.

We discuss the changes in centriole position during the cell cycle, mechanisms of spindle orientation, and how the maintenance of polarized plasma membrane domains through mitosis may facilitate the rapid reformation of the polarized interphase cytoplasm.

During embryogenesis, proper orientation of cell divisions is essential to morphogenesis of the whole embryo. The same holds for tissue regeneration in adults where cell division should occur in the context of neighboring cells to maintain the function of the tissue. It is well established that the axis of cell division is perpendicular to and bisects the axis of the spindle (Rappaport, 1986). The mechanism of spindle orientation in growing tissues is largely unknown, but may involve astral microtubules during prophase and the actin network (Allen and Kropf, 1992; Hyman and White, 1987; Palmer et al., 1992). In certain instances, the spindle attaches to a specific site on the cell cortex (Hyman, 1989; Lutz et al., 1988). Orientation of the spindle axis is not only essential for directional growth but it is also important for cell differentiation. There are many cases of asymmetric divisions where the daughter cells have distinct fates due to partitioning of cytoplasmic determinants (for example Allen and Kropf, 1992; Sulston et al., 1983; Zachson, 1984).

In epithelial tissues, the plane of cell division is not random; cytokinesis can be either parallel or perpendicular to the plane of the epithelium, but rarely at an oblique angle (for review see Wright and Alison, 1984; but see also Lamprecht, 1990). The orientation depends on the type of epithelium and/or time of development. If the cleavage plane is parallel to the plane of the epithelium, one of the daughter cells is lost from the monolayer either apically or basally. This serves several functions as in the generation of the stratified epithelia in mouse embryos (Smart, 1970*a*,*b*) or as a mechanism for maintaining constant cell number in the presence of continuing mitosis (discussed in Wright and Alison, 1984). If the plane of division is perpendicular to that of the epithelium, both daughter cells may remain in the mono-

Address all correspondence to Dr. Sigrid Reinsch, European Molecular Biology Laboratory, Meyerhofstrasse 1, Postfach 10.2209, D69012 Heidelberg, Germany. Telephone: 49-6221-387403; FAX: 49-6221-387306.

layer, leading to two dimensional growth of the epithelium (Ferguson, 1988; LeBlond et al., 1966). Therefore epithelia represent a case study to examine spindle orientation in relation to differentiated neighboring cells and to the internal structure of the cytoplasm established during interphase.

During interphase, the membranes and the cytoskeleton are polarized along the apico-basal axis. Microtubules are organized in stable longitudinal bundles with their minus ends oriented apically and plus ends extending basally (Bacallao et al., 1989). An intact microtubule network is essential for the directed transport of membrane proteins to and from the apical and basolateral plasma membrane domains (Rodriguez-Boulin and Nelson, 1989; Simons and Wandinger-Ness, 1990). The centrioles are located just below the apical plasma membrane. It is not clear whether they nucleate cytoplasmic microtubules (Bré et al., 1987). The centrioles are separated and do not appear to organize the cytoplasmic microtubules, although one centriole functions as a basal body for the primary cilium which extends above the apical membrane (Bacallao et al., 1989; Buendia et al., 1990). Tight junctions, which determine a boundary between the apical and basolateral plasma membrane domains, are maintained during mitosis (Ferguson, 1988; Jinguji and Ishikawa, 1992; Lütcke et al., 1987; Sandig and Kalnins, 1990; Soler et al., 1993), and there have been a few reports that plasma membrane proteins maintain their polarized distribution during mitosis (Tamaki and Yamashina, 1991; Bartles and Hubbard, 1986). Therefore during mitosis some aspects of cell polarity are maintained while the cytoskeleton undergoes dramatic changes to organize a mitotic spindle and carry out cytokinesis.

We have examined cell division in epithelial cells which are maintained under conditions that allow the development of several characteristics specific to the differentiated phenotype. MDCK cells, of kidney origin, develop apico-basal polarity and carry out the directional transport of solutes when cultured on permeable filter supports. We show that even when these cells reach a fairly confluent and highly polarized state, they continue to divide at low frequency. Using immunofluorescence and confocal microscopy, we show that during cell division, the spindles become oriented parallel to the filter substrate and localized in the apical part of the monolayer. Junctions remain intact and membrane proteins stay segregated to the apical and basolateral domains during cell division. During cleavage furrow formation, adherens junctions form immediately between the two daughter cells. In this way, the epithelium grows only in two dimensions and the barrier between the apical and basolateral media is maintained at all stages of mitosis.

Materials and Methods

Cell Culture

MDCK strain II cells were used for all studies. The cells were passaged as previously described (Balcarova-Stander et al., 1984).

Polarized cells were grown on polycarbonate filters (transwell 3412; Costar, Cambridge, MA) with a 0.4-μm pore diam and 24-mm filter diam. Cells were plated at an initial density of $5.5 \times 10^5/cm^2$ (2.5×10^6/filter) and cultured in large dishes with polypropylene filter supports (4 filters/13.5 cm diam petri dish). MEM supplemented with 2 mM glutamine, 5% FCS, 100 U/ml penicillin, and 10 μg/ml streptomycin was added to the apical (2.5 ml) and basolateral (85 ml) surfaces for the filters. The cells were incubated at 37°C in a 5% CO_2 humidified atmosphere for 3 d before fixation and processing for immunofluorescence. We found that the localization of the 114-kD antigen was dependent on particular culture conditions. That is, when cells were plated under conditions where the medium could acidify overnight (i.e., in 6-well plates), the apical localization of this protein was diminished and much of the protein was found on the basolateral surfaces. (Culturing in 6-well plates also affected transcytosis assays.) We therefore limited our studies to cells grown under conditions where the medium would not be depleted or become acidified overnight.

Antibodies

The rabbit polyclonal antiserum raised against a *Xenopus* γ-tubulin fusion protein (Stearns et al., 1991) was the kind gift of Dr. Tim Stearns (Stanford University, Palo Alto, CA) and used at 1:100 dilution. The mouse monoclonal antibodies, RR1, directed against E-cadherin (Gumbiner and Simons, 1986), 4.6.5a, directed against the 114-kD antigen (Balcarova-Stander et al., 1984), and 6.23, directed against the 58-kD antigen (Balcarova-Stander et al., 1984) were provided by Dr. Kai Simons (EMBL, Heidelberg) and were used as neat culture supernatants. Mouse monoclonal antibody directed against β-tubulin (Amersham) was used at 1:250 dilution. Rat monoclonal antibody directed against BrdU (Sera-Lab, Cambridge) was used at 1:100 dilution. The rat monoclonal antibody R26.4C directed against Z0-1 was used as neat culture supernatant and obtained from the Developmental Studies Hybridoma Bank (see acknowledgments section).

Fluorescent derivatized secondary antibodies (Donkey anti-rat, mouse, and rabbit), biotin-labeled goat anti-rat, and FITC streptavidin were purchased from Dianova (Hamburg, Germany), and titered before use on cells grown on glass coverslips.

Fixation

Cells that were stained for β-tubulin or γ-tubulin were fixed using a slight modification of the pH shift method of paraformaldehyde fixation as described in Bacallao et al. (1989) as follows. Filters were rinsed first in PBS with 1 mM Ca^{2+} and 0.5 mM Mg^{2+} (PBS+), and then in microtubule-stabilizing buffer (MTBS[1]; 80 mM K-Pipes, pH 6.5, 5 mM EGTA, 2 mM $MgCl_2$), both warmed to 37°C. The cells were incubated for 5 min at room temperature in 3% paraformaldehyde (Merck GmbH Darmstadt, Germany) in MTSB added to both the apical and basolateral surfaces of the filter. This solution was replaced with 3% paraformaldehyde, 100 mM NaB_4O_7, 0.25% saponin (Sigma), and incubated for an additional 5 min at room temperature. The filters were rinsed briefly with PBS and quenched by incubating for 15 min in 1 mg/ml $NaBH_4$ freshly dissolved in PBS (adjusted to pH 8 with NaOH). The filters were washed with PBS and blocked for 1–2 h at room temperature (or overnight at 4°C) in PBS containing 1% BSA and 0.1% Triton X-100.

Cells stained for E-cadherin, the 58-kD antigen and the 114-kD antigen were rinsed in PBS+ warmed to 37°C, and then fixed in PBS, 3% paraformaldehyde for 30 min at room temperature. Filters were rinsed in PBS and quenched with PBS, 50 mM NH_4Cl, 20 mM glycine for 15 min. Blocking was performed in PBS, 0.2% gelatin (Amersham) for 1–2 h at room temperature or overnight at 4°C.

Cells stained for ZO-1 were rinsed in PBS+ warmed to 37°C, and fixed in methanol at −20°C for 15 min. Filters were then rinsed in PBS and blocked in PBS containing 1% BSA and 0.1% Triton X-100.

Immunofluorescence Staining

Filters were cut from the plastic filter holders and divided into small rectangles with an orientation mark in one corner. Antibodies diluted in the appropriate blocking buffer were added to both sides of the filter pieces. Primary antibody incubations were performed overnight at room temperature or for 1–2 h at 37°C. Incubations were done on parafilm in a small humidified chamber sealed with parafilm. For β-tubulin, we found that an additional incubation in fresh antibody was necessary for complete penetration of the sample. The filters were washed for 15–30 min in PBS, and incubated in secondary antibody diluted in blocking buffer for 1–2 h at 37°C as above. In general, samples were fixed after this step in 4% paraformaldehyde in PBS for 30 min at room temperature, quenched in PBS, 50 mM NH_4Cl for 30 min. Nuclear staining of filters fixed and processed for β-tubulin or

1. *Abbreviations used in this paper*: BrdU, bromo-deoxyuridine; MTSB, microtubule stabilizing buffer.

γ-tubulin was performed directly as described below, while filters stained for membrane antigens were first permeabilized at this step in PBS, 0.1% Triton-X-100, 1% BSA for 15 min, and then processed for chromatin staining.

For staining of chromatin, filters were incubated for 30 min at room temperature in 1 mg/ml RNAseA (Sigma, dissolved in PBS and heated to 95° for 15 min to inactivate contaminating DNAse), and then with 0.1 μg/ml propidium iodide (Sigma, diluted in PBS from 5 mg/ml stock in DMSO) for 15–30 min at room temperature. Filters were washed twice for fifteen minutes each in PBS before mounting.

Specimens were mounted with cells facing upwards on glass slides with two spacers cut from 50-μm thick polypropylene. A drop of 50% glycerol, PBS, 100 mg/ml 1,4 diazabicyclo-(2.2.2) octane (Sigma) was placed on the cell side of the filter and a glass coverslip was carefully lowered onto the spacer supports. The mount was sealed with nail varnish.

Simultaneous Visualization of BrdU-labeled Cells and γ-Tubulin

To determine the optimal timing for locating cells that were in G2-phase and the cell-cycle timing from S-phase to mitosis, filter-grown cells were pulsed with 80 mM bromodeoxyuridine (BrdU) added to the basal compartment of the filter well for 1 h. Cells were washed three times with medium, incubated for varying amounts of time, rinsed briefly with warmed PBS+, fixed for 10 min with 0.3% glutaraldehyde, MTSB, 0.1% Triton X-100, and quenched 30 min in 1 mg/ml $NaBH_4$ freshly dissolved in PBS (adjusted to pH 8 with NaOH). 1.5 N HCl was added to the filters to denature the DNA and incubated for 30 min at room temperature. Filters were rinsed in PBS, blocked for 1 h in MTSB, 0.1% Triton X-100, 1% BSA, and incubated overnight at room temperature in monoclonal rat anti-BrdU. Filters were subsequently washed 30 min in PBS, and incubated in FITC-derivatized donkey anti-rat antibody (Dianova, Immunotech, Hamburg, Germany). Filters were counterstained for chromatin with propidium iodide as above. The percentage of BrdU-labeled cells was between 10–20% for all samples. For an enrichment in G2 cells labeled with BrdU, we determined the chase time where most BrdU-labeled cells had likely completed S-phase, but where the number of BrdU-labeled cells which had entered or completed mitosis was still low. We considered that all interphase cells located in pairs with equivalent BrdU staining were cells which had already completed mitosis and entered G1, and were therefore eliminated from our analysis. By 8 h after labeling, 50% of the BrdU-labeled cells had entered mitosis. We therefore considered this time point as optimal for an enrichment of G2 cells labeled with BrdU, and used cells fixed at this time point for determining the centriole position with simultaneous BrdU and γ-tubulin immunofluorescence as described below. While some of the BrdU-labeled cells (which had not been eliminated as G1 cells) with interphase chromatin could still be completing S-phase, most cells had likely completed S-phase and were preparing to enter mitosis.

For simultaneous γ-tubulin and BrdU detection, cells were fixed with formaldehyde using the pH shift method, processed for γ-tubulin staining as described above including post-fixation and quenching, and then processed for BrdU immunofluorescence as described above omitting the propidium iodide counterstain.

Fluorescence Microscopy

Epifluorescence microscopy for quantitation of centriole position in telophase cells was performed on a microscope (Axiophot; Carl Zeiss, Inc.) equipped for standard epifluorescence microscopy. Confocal fluorescence microscopy was performed with the confocal scanning laser beam microscope (CCM) developed at the European Molecular Biology Laboratory (Stelzer et al., 1989). Either of two objectives was used for imaging: 100X Plan-Apochromat (Zeiss, NA 1.4) or 100× Plan-neofluor (Zeiss, NA 1.3). The 529 and 488 laser lines of an Argon-ion laser (Spectra-physics) were used for excitation of rhodamine/propidium iodide and fluorescein-labeled samples, respectively.

Image Acquisition, Processing, and Data Analysis

Confocal series of mitotic cells were collected at 0.5 or 1 μm steps. The laser power, high voltage (photomultiplier sensitivity), and number of averages (usually 16) were all variable and adjusted to generate images with sufficient contrast. Images were stored on a computer and transferred by ethernet to a Macintosh Quadra. Image analysis was performed using the NIH Image public domain program. Series were reconstructed using the "stack" function allowing distances and angles between the centrioles to be measured in three dimensions.

Images for figures were contrast enhanced in the NIH image program and copied to Canvas (Deneba Software, Miami, FL) for final graphic presentation. Figures were digitally printed using a dye sublimation printing process.

Electron Microscopy

Cells grown on polycarbonate filters were fixed, embedded, sectioned, and photographed as previously described (Parton et al., 1989).

Results

In a Polarized Confluent Monolayer, Cells Continue to Divide at a Low Rate

When MDCK cells are plated on permeable filter supports at or near confluent density, junctions begin to form within a few hours and the cells soon become polarized (Balcarova-Stander et al., 1984). We found that one day after plating, the monolayer had a measurable transepithelial resistance even though the cells continued to divide, the mitotic index being roughly 2%. In this study, we used cells three days after plating when the mitotic index had dropped to 0.2% and the cell density was 10^6 cells/cm^2. Interphase cells in our samples had an average height of 13 μm, an average diameter of 10 μm and fully polarized cells formed a tightly packed epithelium on the filter support. Fig. 1, *a* and *e* shows confocal images of such a monolayer culture stained with an antibody directed against β-tubulin. The cell in metaphase was surrounded by tightly packed interphase cells showing the apical dense microtubule network previously described by Bacallao et al. (1989).

Mitotic Spindles Are Oriented Parallel to the Plane of the Monolayer

In our initial studies, staining for microtubules indicated that mitotic spindles were oriented parallel to the plane of the monolayer as shown in Fig. 1, *a* and *e*. Since the position and orientation of the spindle dictates the site of cleavage plane formation, mitosis in these cells would generate daughter cells remaining within the monolayer. The high magnification view (Fig. 1 *f*) of the metaphase chromatin, and centrioles stained with an antibody directed against γ-tubulin, clearly shows that both spindle poles were contained within a single confocal section. The confocal microscope used in this study generates single confocal sections with an axial depth of 0.7 μm, or roughly 5% of the total cell height. The X/Z (longitudinal) images of a typical metaphase cell and adjacent interphase cells (Fig. 1, *g* and *h*) further clarifies the position of the spindle relative to the adjacent interphase cells. Simultaneous visualization of chromatin and γ-tb (Fig. 1 *g*) indicated that the interphase nuclei were located at the bottom of the interphase cells while the metaphase chromatin extended the full height of the monolayer. The spindle poles (γ-tubulin) were located in a plane parallel to that of the monolayer and just above the adjacent interphase nuclei. The corresponding microtubule staining is shown in Fig. 1 *h*.

It is important for the reader to understand the changes between interphase and mitosis in the microtubule cytoskeleton and in the position of the nuclei and centrioles. The interphase centrioles and microtubules (including primary cilia)

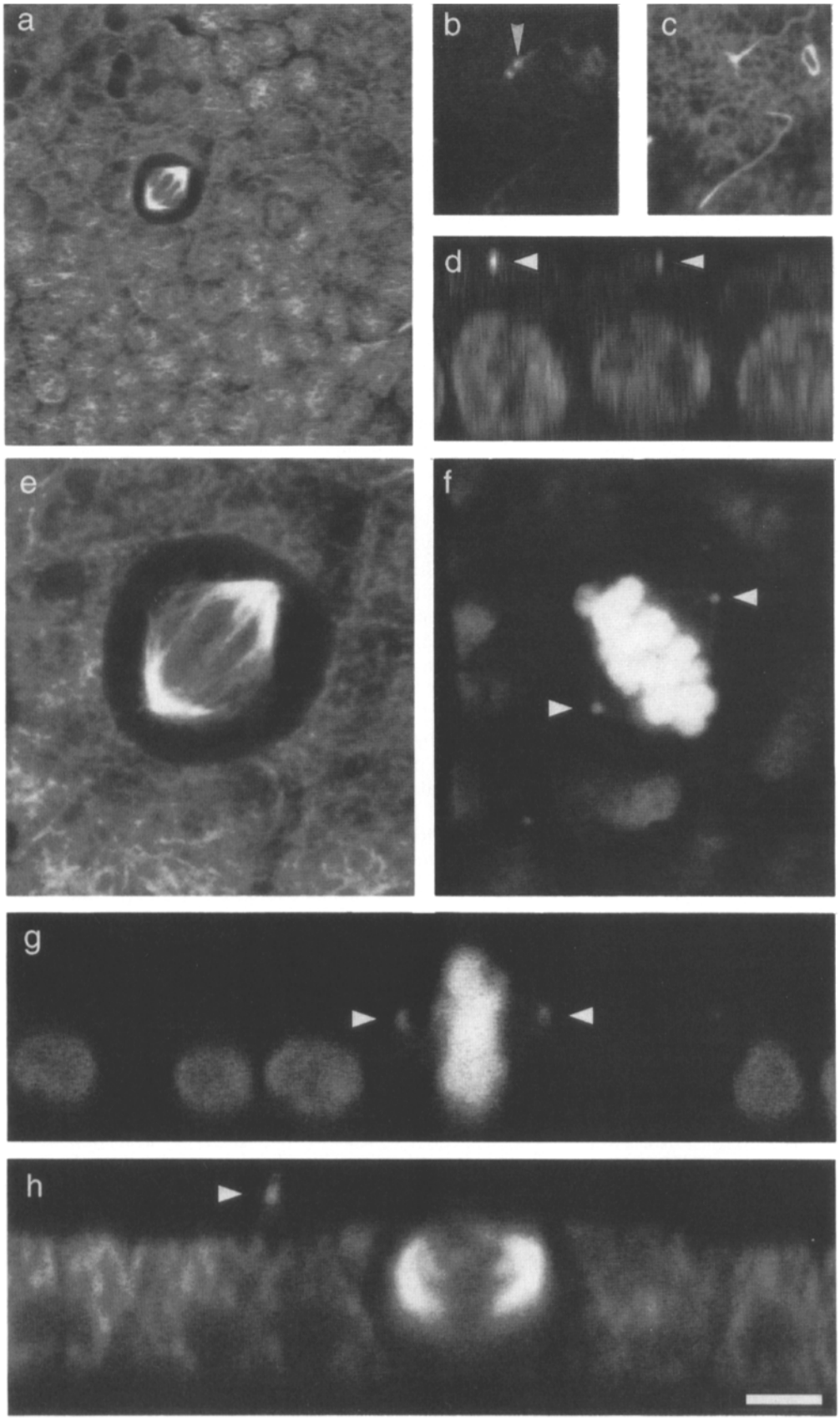

Figure 1. Mitosis in polarized MDCK cells. Cells were plated on permeable filter supports and grown for 3 d before fixation and staining with β-tubulin and γ-tubulin (centrioles) antibodies. Nuclei were stained with propidium iodide. Using confocal microscopy, nuclei and centrioles were visualized simultaneously with a rhodamine filter set (*b*, *d*, *f*, and *g*), while microtubules were visualized in the fluorescein channel (*a*, *c*, *e*, and *h*). (*a*) Low magnification X/Y view of a field of polarized cells with a single cell in mitotic metaphase. The microtubule staining in the surrounding cells is the apical dense network. (*b* and *c*) Apical section of interphase cells shows typical paired but separated centrioles, one of which (*arrowhead* in *b*) serves as the basal body for the primary cilium (revealed by β-tubulin staining in *c*). (*d*) X/Z confocal section to show nuclei and γ-tubulin staining in interphase cells. Nuclei are basal while centrioles (*arrowheads*) are apical. (*e* and *f*) Higher magnification X/Y views of the metaphase cell shown in *a*. Both spindle poles (*arrowheads*) are clearly visible in a single confocal section. The spindle is centrally located within the mitotic cell. (*g* and *h*) X/Z sections of another mitotic cell to reveal centrioles and nuclei (*g*) and microtubules (*h*). Note how the nuclei are aligned at the basal portion of the cell, that the spindle poles are oriented parallel to the substratum and that the metaphase chromatin sits above the level of the surrounding nuclei. Arrowhead in *h* shows part of a primary cilium extending above the monolayer. Bar (*a*) 20 μm; (*b–h*) 5 μm.

are shown in an apical confocal cross-section in Fig. 1, *b* and *c*. The centrioles were usually separated, and the mother centriole (*arrowhead* in Fig. 1 *b*) served as the basal body for the primary cilium which extended above the apical membrane (Fig. 1 *c*). No other apical microtubules were focused at the centrioles. Note also that we did not find staining with the γ-tubulin antibody in the interphase cells in other locations than at the centrioles (Fig. 1, *b* and *d* and Fig. 6 *g*). A longitudinal section (Fig. 1 *d*) showed the relative interphase positions of the centrioles at the apical membrane and nuclei in the basal domain.

To further characterize whether spindles were oriented in the plane of the monolayer in all cells, 51 mitotic cells were analyzed by confocal microscopy. Classification of the cell cycle position was based on the degree of condensation and configuration of the chromatin. Serial confocal sections were taken of each cell, individual cells were reconstructed and the measurements shown graphically in Fig. 2 were made on the reconstructed images as detailed in Materials and Methods. Measurements made on interphase cells in a random field are shown for comparison. Fig. 2 *A* shows that the distance between the two centrioles increased during mitosis. The metaphase pole separation of 10 μm corresponded to one interphase cell diameter, while the average diameter of the metaphase cell at the plane of the spindle poles was 14 μm (data not shown, but see Fig. 1, *e* and *f*). In prometaphase, the axis passing through the two centrioles showed no preferred orientation (Fig. 2 *B*). However, in 8 out of 10 metaphase cells the spindle axis was constrained within 10° of the plane parallel to the monolayer. In addition to the ten metaphase cells analyzed by confocal series and three-dimensional reconstruction, 10 out of 11 metaphase cells on which only single sections were recorded had spindle poles contained within a single confocal section (therefore also under 10°). This analysis indicated that spindle orientation parallel to the plane of the monolayer was tightly controlled in these cells. Spindle orientation was maintained through anaphase and early telophase during which time the centrioles separated to an average distance of 17 μm. The vertical position of the spindle within the cell (Fig. 2 *C*) was analyzed in 56 cells. A line was drawn connecting the two centrioles and the distance between the midpoint of this line and the base of the monolayer was measured and expressed as a percentage of the total monolayer height. In prometaphase, metaphase and early anaphase, the spindle was located within the monolayer at ~60% of the distance from basal to apical. This corresponds to a final positioning of the spindle poles just above the nuclei of the surrounding interphase cells.

Centrioles Move Away from the Apical Membrane in Prophase

The analysis reported in the previous section showed that the centrioles moved at some point of the cell cycle from the apical membrane towards the nuclei to a final metaphase position on an axis parallel to the plane of the monolayer. In prophase cells we found centrioles at all locations within the cell, including very near the basal membrane. We had noted that many cells with normal interphase microtubule arrays and nuclear staining had one centriole located at the apical membrane while the second centriole was located several microns more basally. We thought that such cells were

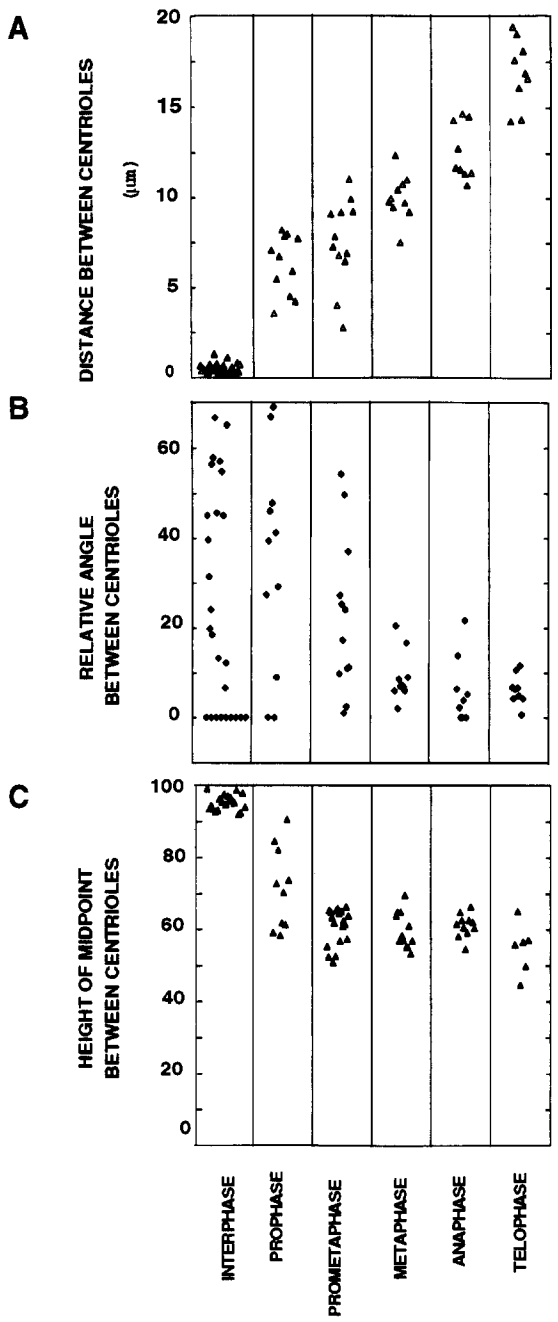

Figure 2. Analysis of centriole movements during the cell cycle. Confocal series of mitotic cells stained for nuclei and centrioles were reconstructed using the NIH image program. Each point represents a measurement from a confocal series on a single cell. (*A*) The distance between the centrioles increases during progression through mitosis. (*B*) Centrioles become aligned in metaphase. The inter-centriolar axis angle was measured relative to the plane of the monolayer (when both centrioles are on an axis parallel to the plane of the monolayer, the angle is 0°). (*C*) Relative height of the centrioles within the monolayer. The midpoint between the two centrioles of the cell was determined and the height of this point above the substratum measured and expressed as a fraction of the total monolayer height. The spindles sit at an average of 60% of the total height of the monolayer as measured from basal to apical.

preparing to enter mitosis and that one centriole had begun its migration toward the nucleus. Since these cells lacked condensed chromatin, we thought that centriole migration could start during the S-G2 phase of the cell cycle. We therefore set out to determine whether centriole migration occurred before chromatin condensation (prophase). Unfortunately we could not use methods such as cell synchronization as this would affect the integrity of the monolayer. However, we reasoned that if centriole migration away from the apical membrane occurred before mitosis, that is in S-phase or G2, we could detect the change in centriolar position in cultures that were pulsed with BrdU (to label S-phase cells) and chased for varying amounts of time. We found that 5–10% of the cells incorporated BrdU after a 1-h pulse and the first BrdU-positive mitotic figures were seen after a 1.5-h chase. This corresponded to a minimum length of 1–2 h for the G2 phase if the first mitotic cells had incorporated the BrdU just at the S/G2 boundary. After an 8-h chase period, 50% of the BrdU-positive cells had entered mitosis. At this 8-h timepoint we could identify several different staining patterns for BrdU which were indicative of cell cycle time. Mitotic cells were clearly identifiable based on chromatin condensation. Paired daughter cells (early G1) could be distinguished since the BrdU staining was equivalent in the two daughters. These had incorporated BrdU in the previous cell cycle and completed mitosis. The remaining BrdU-positive cells which did not have condensed chromatin were presumed to be in late S-phase or G2 and therefore "pre-mitotic". In general, the nuclei of these cells were larger than the surrounding cells which had not incorporated BrdU. Confocal series were collected from 57 premitotic cells (BrdU-positive, not in pairs, chromatin not condensed). The intercentriolar distance and axis were measured, plotted, and compared with 100 random interphase cells (Fig. 3). The distances between centrioles were comparable between the two populations (data not shown). Likewise, in both sets, almost all cells analyzed had at least one and often both centrioles located at the apical membrane with a maximum intercentriolar distance of 4 μm. Cells in which the axis between the centrioles was 1–10° had both centrioles located at the apical membrane but at a variable distance of 0–4 μm from one another. Most centrioles in both populations were less than 2 μm apart. Therefore even in cells with an intercentriolar axis of 70°, this represents a vertical distance of 1.9 μm or 14% of the cell height. If centriolar migration began before prophase, we would have expected a large decrease in the population of cells with both centrioles located at the apical membrane (0–10° axis) and a corresponding increase in the number of cells with a larger axis and distance between the centrioles. We conclude that centriole migration from the apical membrane occurs at or just before prophase.

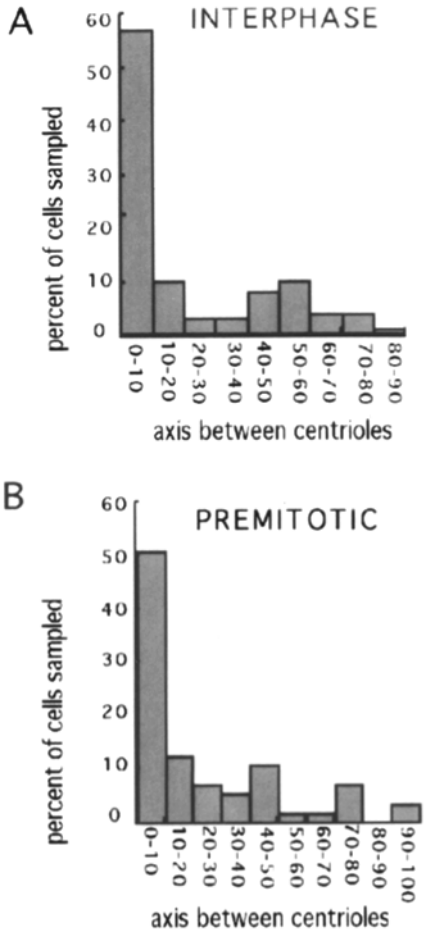

Figure 3. Centriole migration from the apical surface does not occur before prophase. To determine whether centriole migration away from the apical membrane occurs before prophase, premitotic cells were selected by pulse-labeling cultures with BrdU and fixed after a chase period of 8 h. Cells were processed to detect centrioles and BrdU. Confocal series were collected on 50 cells in which the nuclei were labeled with BrdU and the chromatin was not condensed (premitotic cells). Series were reconstructed using the NIH image program and the angle of the axis connecting the two centrioles measured relative to the substratum. In all cells, at least one centriole was attached to the apical membrane. No significant difference in centriole position was noted between the premitotic and interphase cells (100 interphase cells analyzed).

Centriole Movements and Changes in Microtubule Organization in Prophase

Since the analysis in the previous section indicated that the centrioles did not move until prophase, we then set out to characterize the changes in the microtubules, centrioles, and nuclei at prophase onset. Specifically, we wanted to know how the centrioles made contact with prophasic nuclei and when the centrioles became competent to organize a microtubule aster. In prophase, the nuclei were swollen and consumed most of the cytoplasmic space (Fig. 4, *c* and *e*) moving close to the apical membrane. The X/Z images in Fig. 4, *e* and *f* demonstrate that the top of the prophase cell was slightly higher than the surrounding interphase cells. Since in most cases the prophase nucleus had swollen to a great extent and was in close proximity to the apical membrane, we believe that the movement of the centrioles from the apical membrane to the nuclear membrane requires only a short migration, if any, through the apical cytoplasm.

During interphase the two centrioles are different: Only the mother centriole serves as the basal body for a primary cilium (Cohen et al., 1988). However, neither centriole organizes a microtubule aster. In mitosis both centrioles must gain this capacity to serve as spindle poles. We therefore analyzed whether the centrioles differed in their timing for

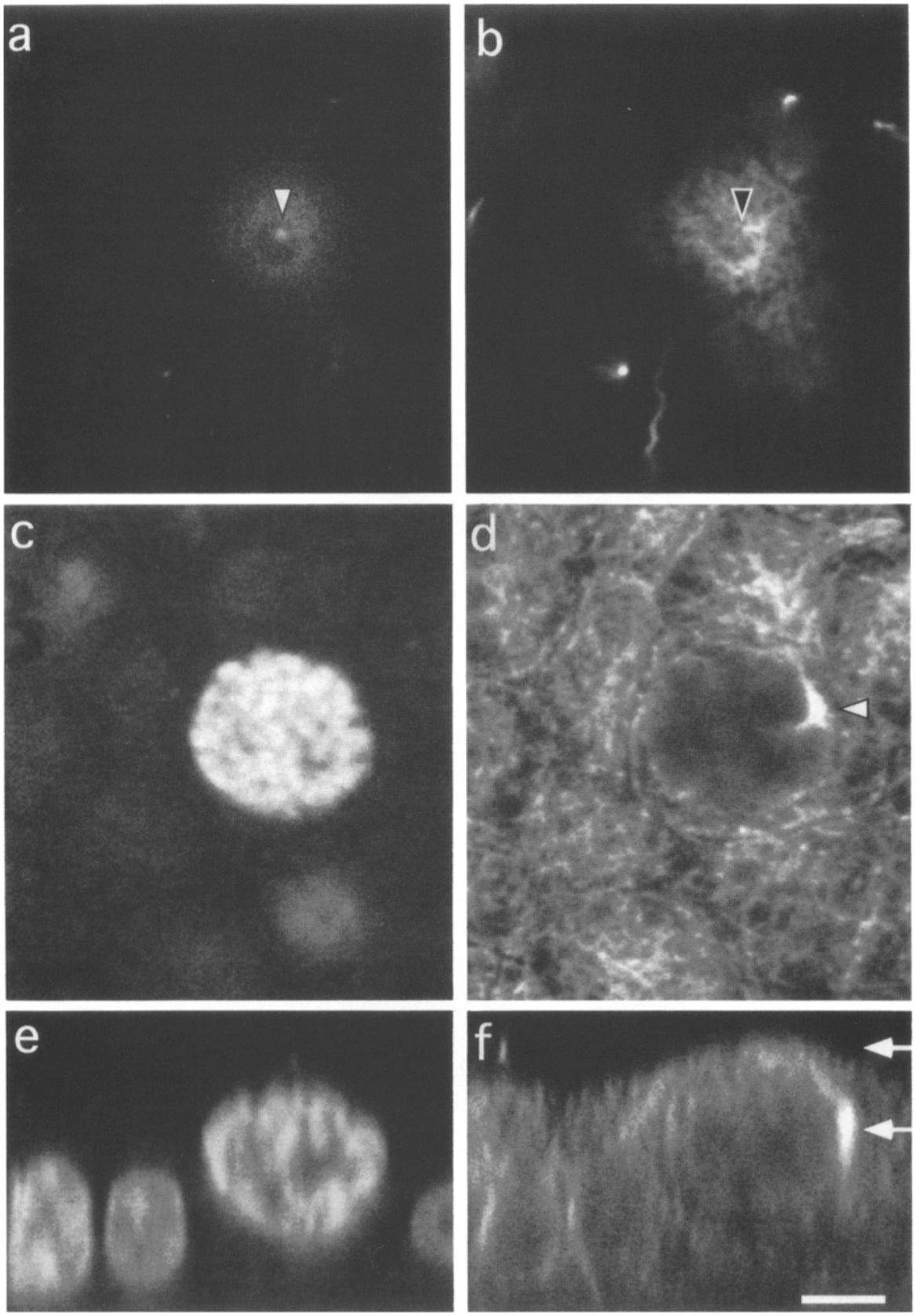

Figure 4. In prophase, migration of the centrioles from the apical membrane correlates with their ability to organize a microtubule aster. (*a*, *c*, and *e*) simultaneous staining for γ-tb and nuclei; (*b*, *d*, *f*) β-tb staining. (*a* and *b*) Apical X/Y confocal sections of an early prophase cell. The centriole (*arrowhead*) in *a* is presumably the mother centriole and the remnant of the primary cilium is visible in *b* (it extends ~1–2 μm to the right from the tip of the *arrowhead*). No cytoplasmic microtubules are organized by this centriole which is still attached to the apical membrane. (*c* and *d*) X/Y confocal sections at the level of the second centriole in the same cell ~3 μm below the apical membrane. The condensed prophase chromatin staining is apparent in *c*. β-Tubulin staining shows the focus of a small aster of microtubules in *d*. (*e* and *f*) X/Z confocal sections of the same cell shown in *a–d*. Note the swollen prophase nucleus which has moved apically from the interphase basal position, and that the top of the prophase cell is higher than the tops of adjacent cells. The arrows in *f* indicate the position of the confocal sections in *a–d*; the upper arrow corresponds to *a* and *b* and the lower arrow to the *c* and *d*. Bar, 5 μm.

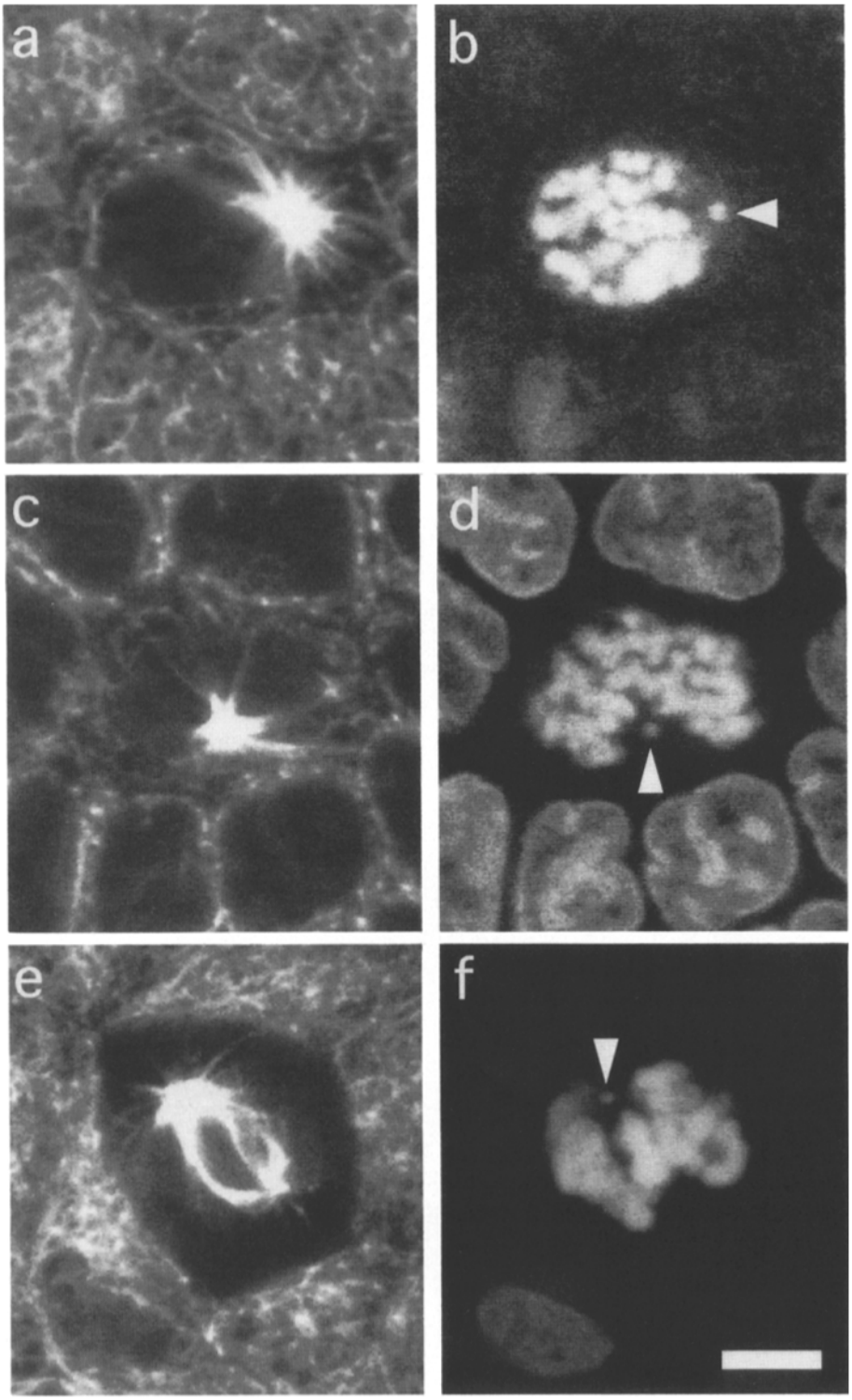

Figure 5. Prophase and prometaphase centrioles have long astral microtubules which contact the cell periphery. Two focal sections of a prophase cell (*a–d*) and a single focal section from a prometaphase cell (*e* and *f*) are shown. (*a*, *c*, and *e*) β-tb. (*b*, *d*, and *f*) Simultaneous staining for centrioles (γ-tb, indicated with *arrowheads*) and nuclei (propidium iodide). Both centrioles in the prophase cell in *a–d* have migrated from the apical membrane and organize extensive asters. The images in *a* and *b* are from a more apical part of the monolayer, while the centriole in *c* and *d* has migrated more basally and the microtubules extend below the prophase nucleus. The interphase microtubule network in the prophase cell has not yet completely disassembled (compare with *e* and *f*). (*e* and *f*) In prometaphase the bipolar spindle has formed but not yet become aligned. A single section is shown here to demonstrate that in prometaphase the astral microtubules are still long and contact the periphery of the cell. The other centriole in this cell was found in a section located 2 μm towards the basal domain of the cell. Bar, 5 μm.

migration away from the apical membrane and in their capacity to organize microtubule asters at prophase onset. Prophase cells were selected by virtue of their condensed chromatin. An analysis of ~30 prophase cells revealed that the timing of association of the two centrioles with the nucleus as well as their ability to organize a microtubule aster at prophase onset differed. The centriole serving as a basal body for the primary cilium remained associated with the apical membrane longer than the other centriole. Fig. 4, *a* and *b* shows the apical most section of an early prophase cell. One centriole (Fig. 4 *a*) was located at the base of a very short primary cilium (*arrowhead* in Fig. 4 *b*), most likely in the process of being resorbed. This centriole did not seem to organize an aster of cytoplasmic microtubules. However, the other centriole had migrated along the side of the nucleus and started to nucleate microtubules (Fig. 4 *d* as well as the X/Z image in Fig. 4 *f*). The interphase microtubule network in the vicinity of this centriole had not yet completely disas-

sembled (compare with the metaphase cell in Fig. 1 and the prometaphase cell in Fig. 5, *e* and *f*). In all early prophase cells with a primary cilium, the centriole still associated with it did not organize a microtubule aster, while that located at the nuclear membrane did. A cell slightly more advanced in prophase is shown in Fig. 5, *a* and *d*. Both centrioles were located at the nuclear membrane in two different confocal sections. Both nucleated large asters with long microtubules which extended to the cell cortex. The long microtubules extended over (Fig. 5 *a*) and beneath (Fig. 5 *c*) the prophase nucleus. Both centrioles were situated in clear indentations in the nucleus. The long astral microtubules persisted through prometaphase (Fig. 5, *e* and *f*) but only a few apparently short astral microtubules were seen at metaphase (Fig. 1, *a* and *e*). We saw the full range of prometaphase chromatin/centriole arrangements described by others (Rattner and Berns, 1976; Roos, 1976; Waters et al., 1993) indicating that the generation of spindle bipolarity likely takes a number of routes.

Centriole Relocation at Cytokinesis

After cytokinesis, the centrioles dissociated from the nucleus and moved back to the apical membrane. To determine whether the centriole migration to the apical membrane during telophase took a particular route, we quantitated the position of the centrioles on a conventional epifluorescence photomicroscope in 150 pairs of newly divided cells where a midbody could still be detected by β-tubulin immunofluorescence. We sorted these into three broad classes based on centriole position relative to the apical/basal axis and the proximal/distal axis (proximal being toward the midbody and distal toward the spindle poles). These classes are shown in Fig. 6. The two most easily defined classes corresponded to cells in early or late telophase. In early telophase cells (Fig. 6, *a–d*, 25% of the daughter cell pairs), the chromatin was still clearly highly condensed and the centrioles positioned distally at the former spindle poles. Typically a distinct band of microtubules circled the periphery of these cells, and microtubules extended from the nuclei toward the midbody (Fig. 6, *b* and *d*). Cells were considered as late telophase (Fig. 6, *g* and *h*, 17% of the daughter cell pairs) when the centrioles in both daughter cells were located at the apical membrane, the chromatin had decondensed significantly, and the interphase microtubule array had largely reformed. The remaining 48% of the telophase cells were considered to be intermediates between these two classes, that is, in mid-telophase. An example of such a cell pair is shown in Fig. 6, *e* and *f*. In this telophase pair, one centriole was located distally and the centriole in the other daughter cell located close to the nucleus proximal to the midbody. In mid-telophase, the position of the centrioles appeared to be more or less random without correlation between two daughter cells. However, they were always very close to the nucleus. A small aster of microtubules was generally associated with each centriole and there were few apical microtubules. Our distinct impression was that the centrioles remained associated with the nuclear membrane until the centrioles achieved an apical position. Our data are consistent with two possibilities. Either the centrioles migrated relative to a stationary nucleus, and that this migration took a number of paths, or the newly formed nuclei rotated before the centrioles dissociated from the nuclei. Such a rotation of the nucleus might have positioned the centrioles fairly close to the apical membrane if the rotation occurred before the cells increased in height at cytokinesis. Centrioles lost the capacity to organize a microtubule aster upon arrival at the apical membrane (Fig. 6, *g* and *h*), at which time the dense apical microtubule network reformed, mother and daughter centrioles separated, and the primary cilium reformed.

Membrane Proteins Remain Polarized during Mitosis

The hallmark of a polarized epithelium is the sorting of plasma membrane proteins into distinct apical and basolateral domains of the cell surface (Simons and Fuller, 1985). These domains are separated by tight junctions which surround the cells just below the apical surface. Since cytoplasmic microtubules play an important role in polarized sorting of plasma membrane protiens and since the interphase microtubule network is disassembled during mitosis, we wondered whether plasma membrane proteins remained properly sorted in mitotic cells.

We characterized the distribution of three antigens in mitotic cells by immunofluorescence and confocal microscopy: uvomorulin (E-cadherin) which localizes to adherens junctions on the basolateral membrane (Gumbiner and Simons, 1986), a 58-kD basolateral protein (Balcarova-Stander et al., 1984) and a 114-kD protein which sorts to apical membranes by a transcytotic mechanism (Balcarova-Stander et al., 1984; Brandli et al., 1990).

E-cadherin was excluded from the exposed apical domain in all cells including mitotic cells. In interphase, E-cadherin was present on the lateral sides of the basolateral membrane (Fig. 7 *D*). No E-cadherin was found in the most basal portion of the membrane which was in contact with the filter support and staining stopped abruptly at the apical-most part of the lateral membrane (Fig. 7 *D*). In prophase as the cells began to round up, and until the end of mitosis, E-cadherin was located on the entire basolateral plasma membrane (Fig. 7, *A–C*). The localization at the basal part of the mitotic cell intrigued us since E-cadherin localizes to adherens junctions, that is, at sites of cell–cell contact. We examined 20 confocal series of mitotic cells to determine whether adjacent cells extended beneath the mitotic cells to form adherens junctions. The boundaries of adjacent cells were tracked through the confocal sections. Neighboring cells were found to extend beneath all mitotic cells examined, though it was difficult to assess whether the mitotic cell still maintained some contact with the filter. The presence of such extensions from surrounding cells beneath the mitotic cell was confirmed at the EM level (Fig. 8, *a* and *b*). This figure also shows several spot desmosomes along the mitotic cell membrane including at the basal side of the cell, and highlights the absence of contact of the basal surface of the mitotic cell with the filter. At the apical border between interphasic and mitotic cells, E-cadherin staining curved over the top of the mitotic cell. E-cadherin was also found in the cleavage furrow (Fig. 7 *C*) indicating that daughter cells form adherens junctions with each other immediately and are not separated by the neighboring cells. We conclude that mitotic cells make adherens junctions on the entire basolateral surface with the surfaces of neighboring interphase cells which curve beneath and over the mitotic cells. This phenomenon

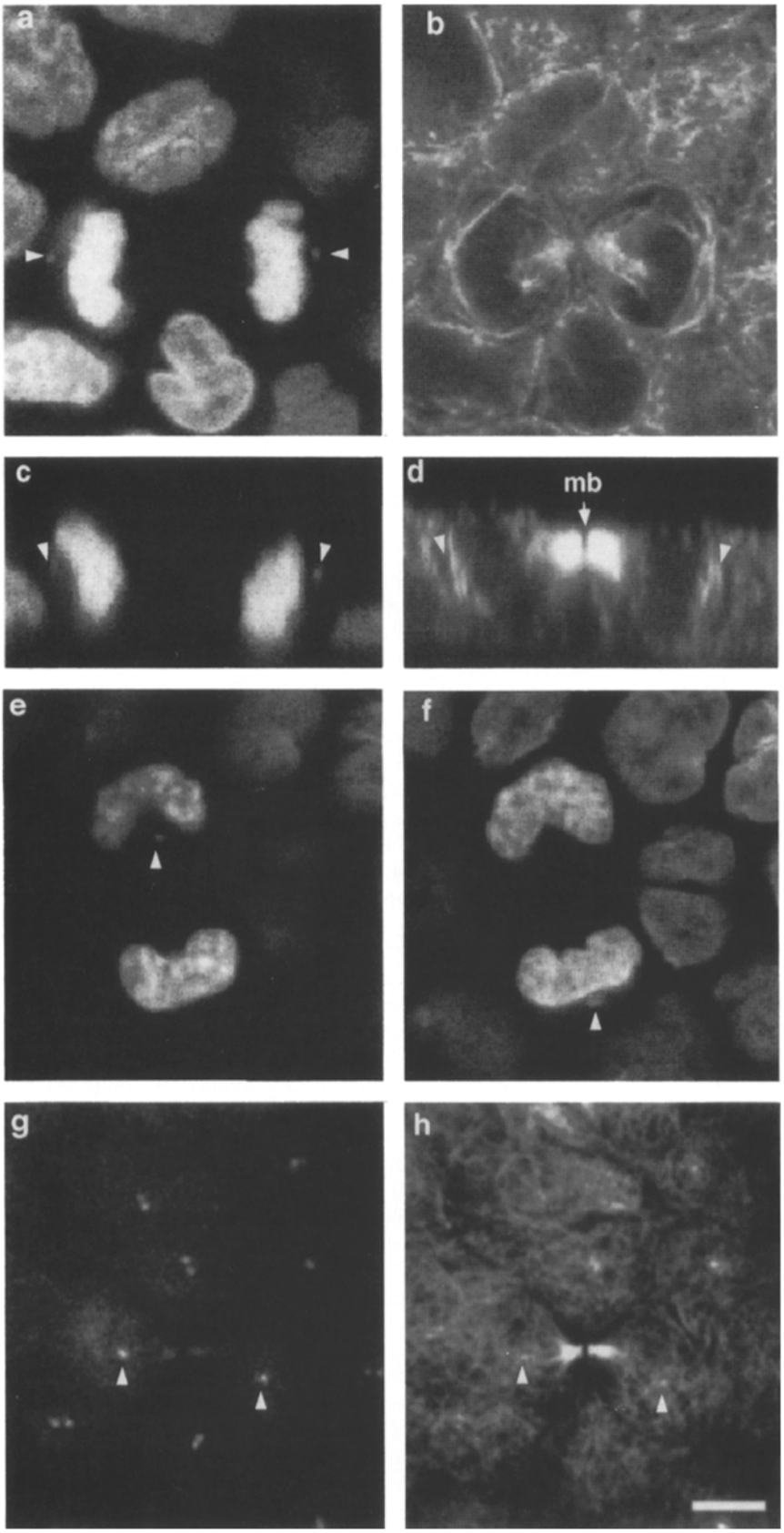

Figure 6. Centriole movements in telophase. (*a*, *c*, *e*, *f*, and *g*) Centrioles (*arrowheads*) and nuclei; (*b*, *d*, and *h*) microtubules; (*a–d*) As nuclei reform in early telophase the centrioles are located away from the midbody; (*a* and *b*) show a single focal plane containing the two centrioles which organize long microtubules extending around the cell periphery. The X/Z images in *c* and *d* show the same cell as in *a* and *b*. In *c*, the γ-tb staining at the centrioles has decreased in intensity from metaphase, and the typical kidney shape of the nuclei is apparent. In *d*, the microtubules of the midbody (*arrow*) are located close to the apical membrane of the cell and extend toward the nuclei. The position of the centrioles is shown by arrowheads. (*e* and *f*) Two focal planes of a mid-telophase cell pair in which the centriole of one daughter cell has moved towards the midbody (*e*) and is slightly more apically located than the centriole in the other daughter cell (*f*). (*g* and *h*) In late telophase, the centrioles have reached the apical membrane, and the interphase apical dense network of microtubules has reformed. Bar, 5 μm.

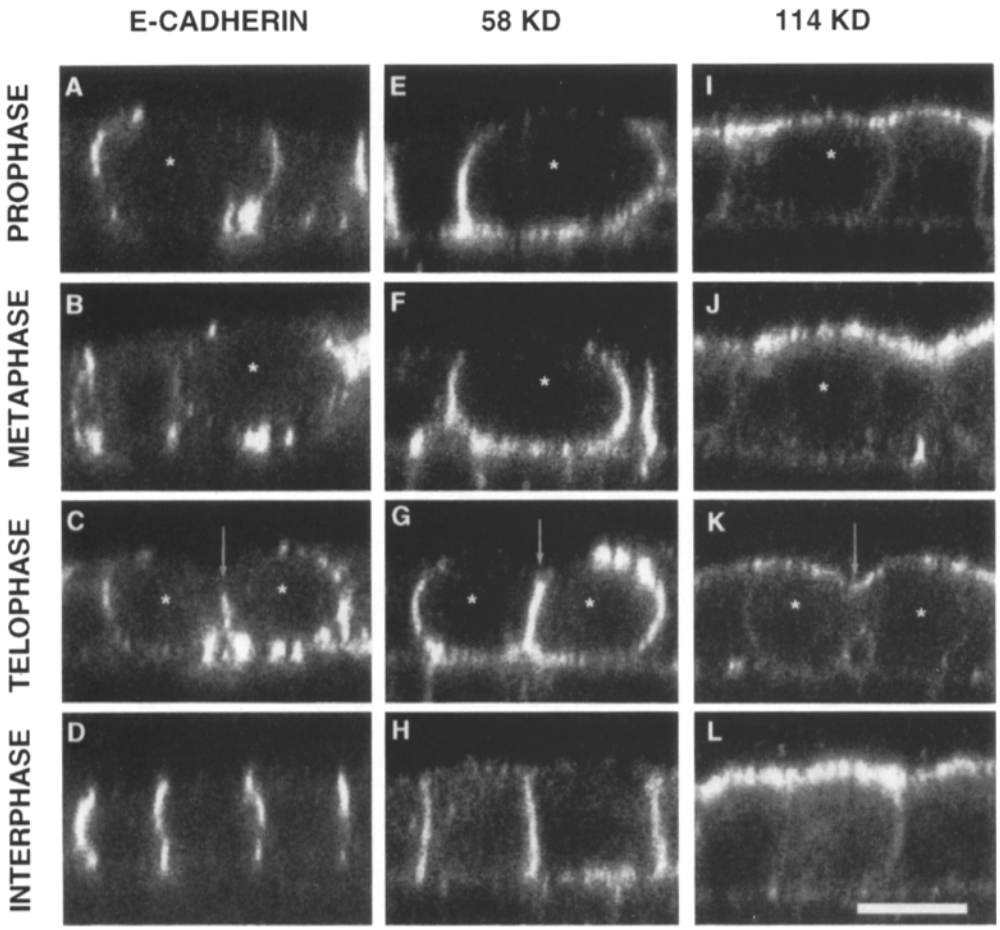

Figure 7. Distribution of membrane polarity markers during mitosis. Staining for these antigens demonstrates that apical and basolateral membrane domains are maintained during mitosis and that the surrounding interphase cells make extensive contacts to the rounded dividing cells. Mitotic cells are indicated (*). The position of the cleavage furrow in *C*, *G*, and *K* is marked by arrows. (*A–D*) Staining for E-cadherin. The staining extends along the baso-lateral membrane at the points of cell–cell contact. Staining is entirely excluded from the apical membrane. Note that the mitotic cells have staining which extends along the basal surface (*A–C*) while the interphase cells (*D*) have staining only on the lateral part of the basolateral membrane. (*E–H*) Staining for the 58-kD basolateral marker protein. Staining extends to all parts of the basolateral membrane in both interphase and mitotic cells. In telophase, cells have bright staining for E-cadherin and the 58-kD antigen at the cleavage furrow. (*I–L*) 114-kD apical marker protein which also faintly labels the basolateral membrane both in interphase and mitosis. Bar, 10 μm.

most likely helps the mitotic cell to stay within the monolayer and may be crucial for the maintenance of the integrity of the epithelium during cell division.

In interphase, the 58-kD antigen localization differed qualitatively from E-cadherin. In addition to the distribution at the lateral membrane, in most cells the 58-kD antigen was also present at the basal surface contacting the filter support (Fig. 7 *H*). There was also some fainter staining detected on the apical domains of all cells, including the mitotic cells. The staining on the basolateral membranes in mitotic cells (Fig. 7, *E–G*) paralleled that of E-cadherin, such that the mitotic cell boundaries were easily viewed, and the "feet" from the surrounding interphase cells which extended below the mitotic cell could be traced through serial sections (data not shown). These results demonstrate that this basolateral protein remains polarized during mitosis and the staining pattern adds support to the contention that surrounding interphase cells extend processes both under and over a dividing cell.

The 114-kD antigen undergoes sorting to the apical membrane via a transcytotic mechanism (Brandli et al., 1990). The staining for this antigen was primarily, though not exclusively, found on the apical membrane both in interphase and mitosis (Fig. 7, *I–L*). The level of expression of this antigen varied from cell to cell in our population (Fig. 10 *b*) giving a rather checkerboard appearance to the apical surfaces of different cells in the monolayer. The staining for this antigen was useful for understanding the shape changes that occur at cytokinesis (see below).

The Tight Junctions Are Maintained during Mitosis

The finding that the three membrane proteins remained polarized indicated that the tight junctions were also maintained during mitosis as has been suggested by others (Sandig and Kalnins, 1990). The staining for E-cadherin and the 58-kD protein demonstrated that the basolateral domain extended very high on the mitotic cells. The tight junctions are located at the boundary between the basolateral domain and the apical domain. We predicted that the apical domains of mitotic cells would therefore be quite small relative to the largest diameter based on the staining for the three membrane proteins. We determined the localization of the tight junction protein ZO-1 in 31 mitotic cells. The tight junctions were maintained during all stages of mitosis. The staining confirmed that the surrounding interphase cells extended projections over the mitotic cells. In areas of the monolayer where cells were of uniform height, the apical domains of

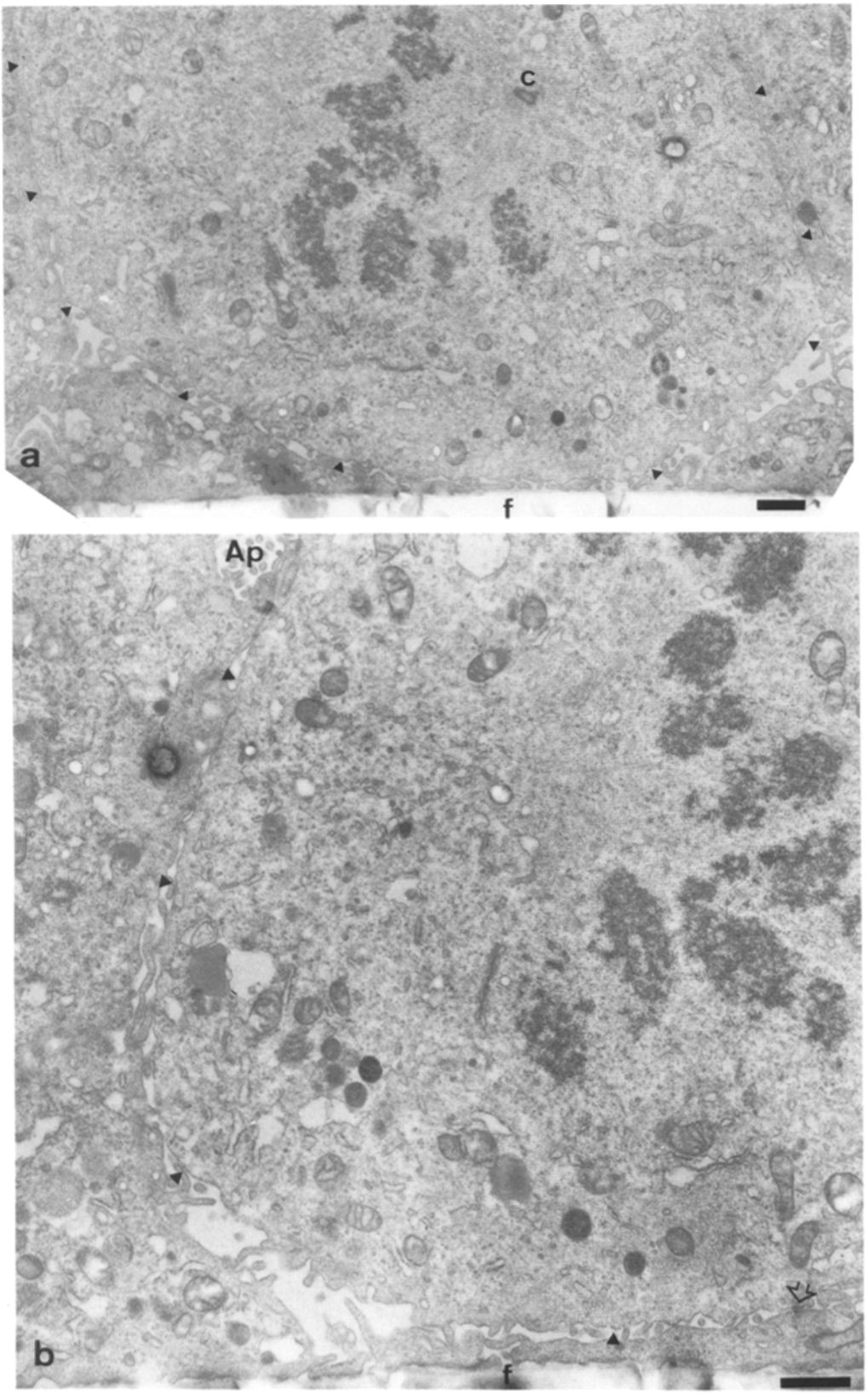

Figure 8. Neighboring cells extend processes beneath the mitotic cell. Two sections from a mitotic cell are shown. Arrowheads indicate the mitotic cell boundaries. The feet from the neighboring cells which extend beneath the mitotic cell are clearly visible in both sections. *Ap*, apical; *c*, centrosome; *f*, filter. The open arrow in *b* indicates a spot desmosome connecting the basal surface of the mitotic cell with the foot from the neighboring cell. Other desmosomes are also visible in *a*. Bar, 1 μm.

interphase cells were similar in area, though somewhat irregular in shape (Fig. 9 *b*). During mitosis, the cross-sectional area of the apical domain (as defined by the ZO-1 staining), appeared smaller and much more irregular in shape (Fig. 9, *e*, *h*, and *k*), while the largest diameter of the cell in the basolateral domain increased relative to the surrounding cells (Fig. 9, *f*, *i*, and *l*). Staining for the 114-kD antigen also confirmed the small size of the mitotic apical membrane (Fig. 10).

Cell Shape Changes at Cytokinesis

During cytokinesis, the surrounding cells remained attached to the mitotic cell at all points along the basolateral membrane. As the spindle poles separated to the maximum telophase distance of 15–20 μm (two interphase cell diameters – Fig. 2 *A*), the cells adjacent to the spindle poles were deformed by this expansion. The tight junctions remained intact (Fig. 9, *j–l*) and appeared to constrain the expansion of the apical domain along the spindle axis. The baslolateral domain expanded horizontally to accommodate the elongating spindle. The telophase apical domains remained small as evidenced by both tight junctional staining and staining for the 114-kD antigen. The apical domains of surrounding interphase cells extended to cover most of the telophase daughter cell diameters. This can be seen both in cross-section (Figs. 9, *j–l*, 10, *a–c*) and in longitudinal section (Fig. 10, *d* and *e*). Therefore, only a very small area of telophase plasma membrane adjacent to the midbody remains exposed to the apical medium.

The cleavage furrow was formed asymmetrically proceeding from basal to apical. As the cleavage furrow progressed apically within the basolateral domain, the midbody (microtubules) also moved apically (Fig. 6 *d*). The apical domain contracted only slightly toward the basal part of the cell during cytokinesis (Figs. 6, *c*, *g*, and *k*, 10, *d* and *e*).

Discussion

The Centriole Cycle in Epithelial Cells

During G1, the centrioles are separated and located at the apical membrane (Fig. 10, Cohen et al., 1988). The mother centriole is attached to the plasma membrane and acts as a basal body for the axoneme of a primary cilium (Fig. 1 *c*). The centrioles do not have asters of microtubules associated with them although they stain for γ-tubulin (Fig. 1 *b*) as has been recently reported in several epithelia (Muresan et al., 1993; Rizzolo and Joshi, 1993 and for review see Joshi, 1993). It is unclear whether they nucleate microtubules. They could nucleate microtubules which are then released and positioned in the cytoplasm through the action of motors (Gelfand and Bershadsky, 1991). Microtubules could also be nucleated by spontaneous assembly due to the presence of microtubule-associated proteins in the cytoplasm (Bré et al., 1987) or by nucleating material located in the apical domain of the cells and separated from the centrioles. We were unable to detect any other localized or diffuse site of γ-tubulin staining in our sample.

The beginning of primary cilium resorption and initiation of centriole replication are concomitant with the initiation of DNA replication (Cohen et al., 1988; Tucker et al., 1992; Vorobjev and Chentsov, 1982). These changes in the centrioles and primary cilium are not correlated with any detectable change in the interphase cytoplasmic microtubule array (data not shown). In G2, the primary cilium reforms again, only to be resorbed at prophase onset. Dissociation of the centrioles from the apical membrane, their association with the nucleus and initiation of microtubule aster assembly all occur in prophase when the chromosomes condense and the interphase microtubule array starts to fall apart (Fig. 11 *b*). This coordinated set of cytoplasmic events is probably induced by cell cycle signals that have been shown to stimulate microtubule severing and increase microtubule nucleation by centrioles in prophase (Karsenti, 1993; McNally and Vale, 1993; Buendia et al., 1992). The centrioles do not organize microtubule asters before they make contact with the nuclei. Swelling of nuclei seems to bring nuclei in contact with the centrioles rather than the centrioles migrating from the apical membrane towards the nuclei (Fig. 11 *b*).

After metaphase, relocation of the centrioles to the apical membrane appears to involve two steps. First, they move to the apical side of the nucleus taking a random route (possibly involving nuclear rotation), and then they migrate to the apical membrane (Fig. 11 *f*). During this migration, they still organize microtubule asters that may help in directing the movement. Therefore, this migration in late telophase may not be the exact reverse process of what happens in prophase. Centriole relocation at cytokinesis similar to that reported here has also been described for fibroblasts in culture (Mack and Rattner, 1993; Moskalewski and Thyberg, 1992).

Spindle Positioning in Polarized MDCK Cells

We found that the final orientation of the spindle parallel to the plane of the monolayer occurs during metaphase and is maintained throughout cytokinesis. There are several possible mechanisms for spindle orientation including determination by (*a*) the long axis of the cell, (*b*) differences in cortical stiffness which displace the spindle to an equilibrium position, (*c*) equal centriole migration, and (*d*) cortical sites for spindle attachment.

The simplest mechanism corresponds to an orientation parallel to the longest axis of the cell (Oud and Ninninga, 1992). In polarized MDCK cells during interphase, the long axis is perpendicular to the plane of the monolayer. However, mitotic cells lose the columnar architecture and round up towards the apical part of the monolayer. Such rounding up of mitotic cells away from the basement membrane is commonly observed in columnar epithelia (Franke et al., 1982; Fujita, 1962). We have not done a detailed morphometric analysis of mitotic cell dimensions in our sample. However, crude measurements indicate that a metaphase spindle could orient in almost any direction within the cytoplasm. It is possible that different regions of the mitotic cortex differ in their stiffness. This could cause unequal forces to be exerted on the astral microtubules by the cortex as proposed by Bjerknes (1986) for the positioning of astral mitotic spindles in early embryogenesis. Clearly, the apical and basolateral domains may differ significantly in cortical stiffness.

In many cells, the spindle position is determined by the separation and migration of the centrioles to opposite sides of the prophase nucleus (i.e., the AB blastomere in *C. elegans*, Hyman and White, 1987). In MDCK cells, a horizontal orientation would be expected if the centrioles, which are apical in interphase, were to migrate an equal distance from

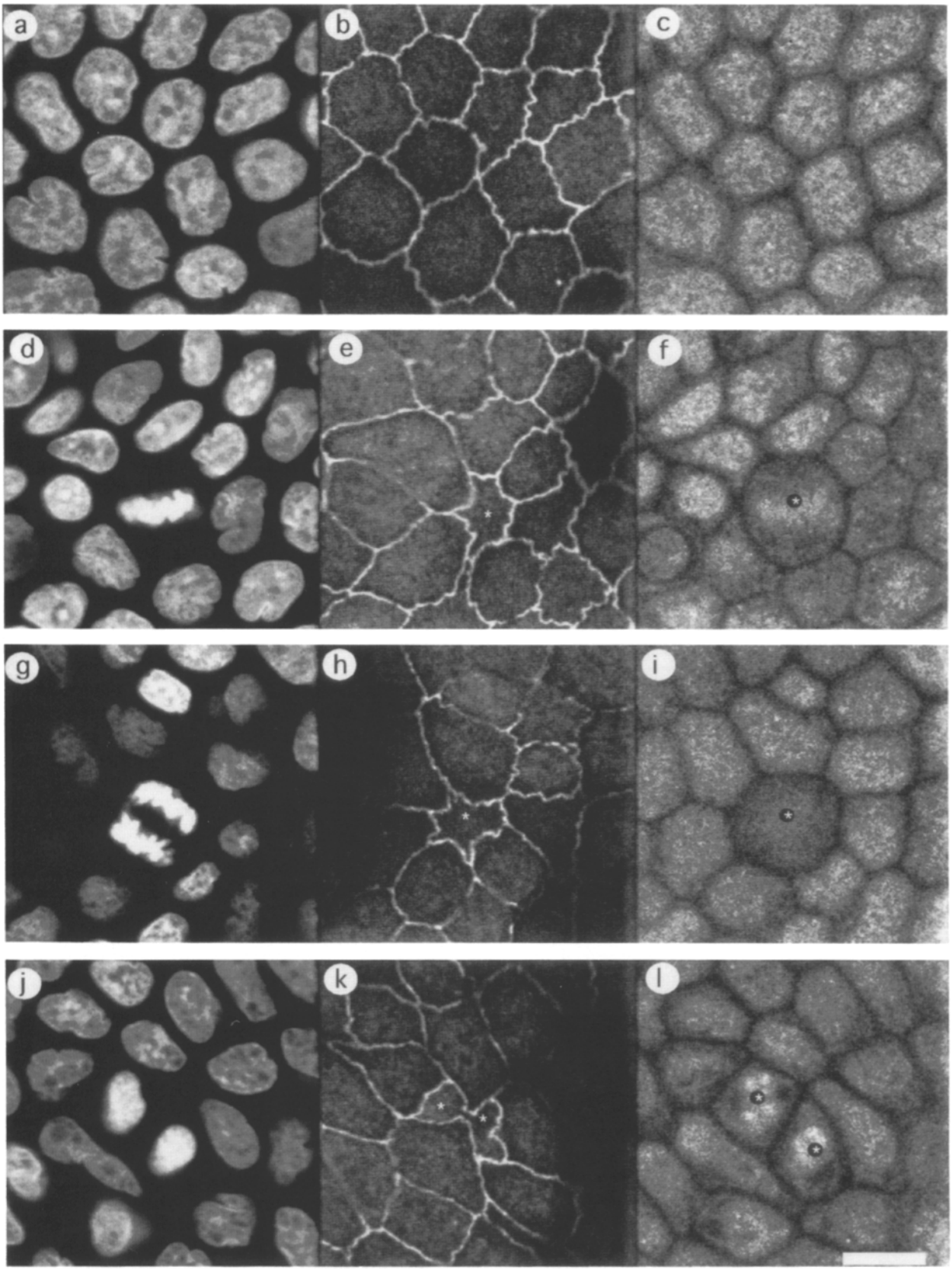

Figure 9. Localization of the tight junction protein ZO-1 during mitosis. Single confocal sections. (*a*, *d*, *g*, and *j*) Nuclei taken at the same position as the largest mitotic cell diameter (shown in *c*, *f*, *i*, and *l*); (*b*, *e*, *h*, and *k*) tight junctions (ZO-1); (*c*, *f*, *i*, and *l*) background staining due to the secondary antibody (*overexposed*) to show cell boundaries at the largest diameter of the mitotic cells. Mitotic cells are marked with asterisks. (*a–c*) Interphase cells. Note the uniform spacing of nuclei in *a*. The apical ZO-1 staining in *b* correlates fairly well with the cell boundaries in *c* indicating that interphase cell boundaries are columnar. Note also how the apical domains (*b*) are fairly

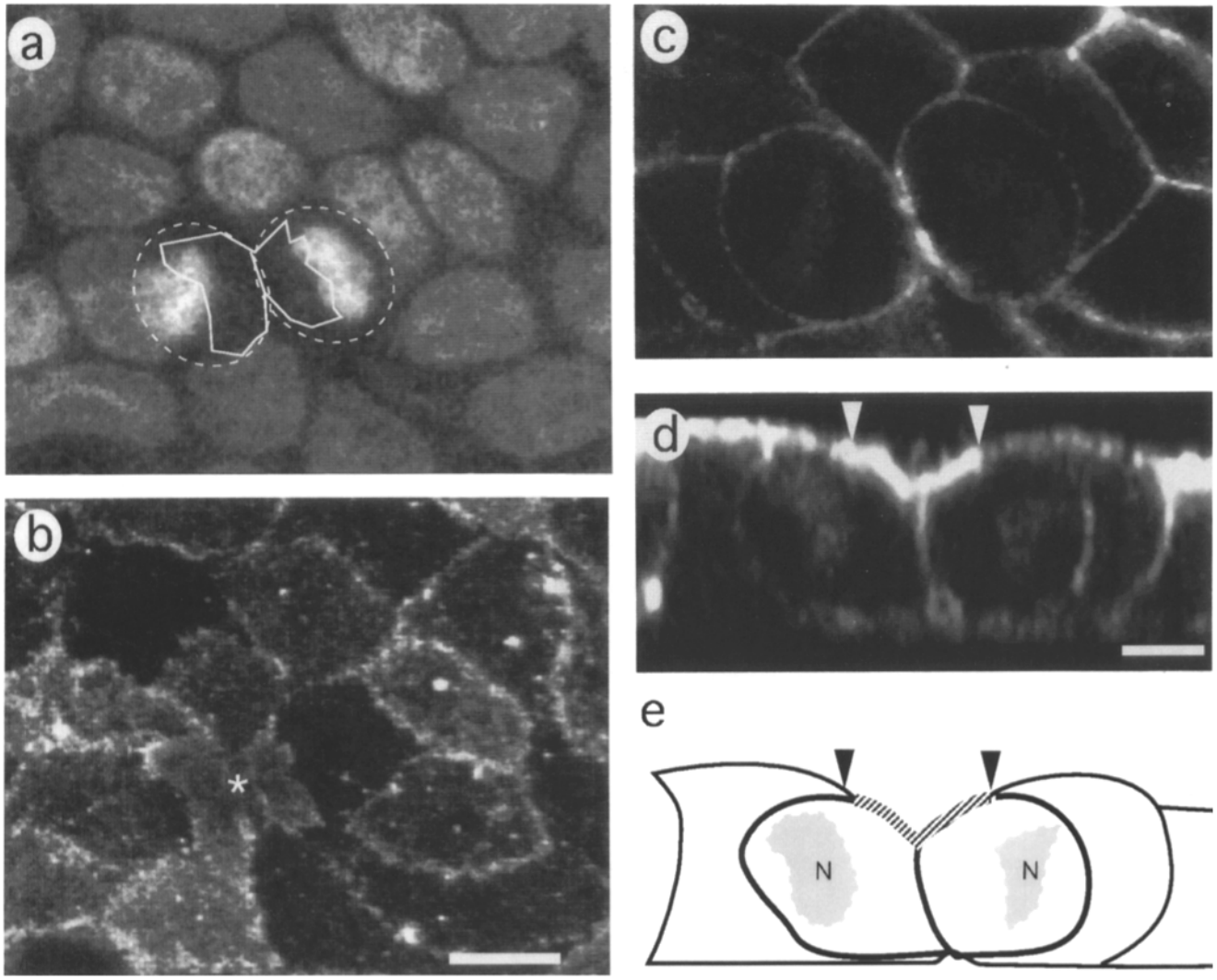

Figure 10. Staining for the 114-kD apical marker protein indicates that surrounding interphase cells extend processes over the telophase cell. (*a*) Projections of multiple X/Y confocal sections to show nuclei (average of 5 confocal sections totaling 2.5 μm vertical depth). The solid line indicates the area of exposed apical surface of the late telophase daughter cell pair (redrawn from panel *b*) while the dotted lines indicate the largest diameter of the pair (redrawn from panel *c*). (*b*) Apical surface staining for the 114-kD antigen (projection of 8 apical confocal sections = 4 μm vertical average). Individual cells express different levels of this antigen on the apical surface which gives a patchwork appearance to the monolayer and allows for the easy identification of cell boundaries. The asterisk in *b* marks the combined apical membrane for the telophase daughter pair. (*c*) A single confocal X/Y section showing the largest diameters of the telophase daughters more basally. This image was digitally enhanced to bring out the basolateral staining for the 114-kD antigen. The basolateral staining for this antigen is much lower than the apical staining (see panel *d*). (*d*) X/Z image of the telophase cells. The arrowheads mark the boundaries of the exposed apical surface where the tight junctions are presumably located. The boundary between the daughter cell on the right and the adjacent interphase cell is especially apparent due to differences in expression of 114-kD protein on the surface. The drawing in *e* is provided for clarification, arrowheads indicate presumed location of the tight junctions, fat dark lines are the daughter cell basolateral membranes, and hatched fat lines are the apical plasma membrane domains of the daughter cells. Bar in *d*, 5 μm and applies to *c–e*. Bar in *b*, 10 μm and applies to *a* and *b*.

the apical membrane to opposite sides around the prophase nucleus and maintain this orientation throughout cytokinesis. Our data on centriole positions in prophase and prometaphase contradict this possibility. The centrioles do not migrate simultaneously and are still not aligned horizontally in prometaphase, confirming previous reports in other systems (Zeligs and Wollman, 1979). Bipolar spindle assembly likely takes several pathways as previously described (Ratt-

uniform in shape and size. (*d–f*) Metaphase. The apical domain of the metaphase cell (*e*) is much smaller than the largest diameter of the cell more basally (*f*). The tight junctions form a continuous boundary around the apical domain which is quite irregular in shape. (*g–i*) The apical domain remains small and irregular shaped through anaphase. By late telophase (*j–l*) the cleavage furrow separates the daughter nuclei basally (*l*), but an intercellular bridge remains and the tight junctions have not yet formed to separate the apical domains (*k*). Note that the apical domains of the daughter cells are still only a fraction of the cross-sectional area at the level of the nuclei (compare *k* and *l*). Bar, 10 μm.

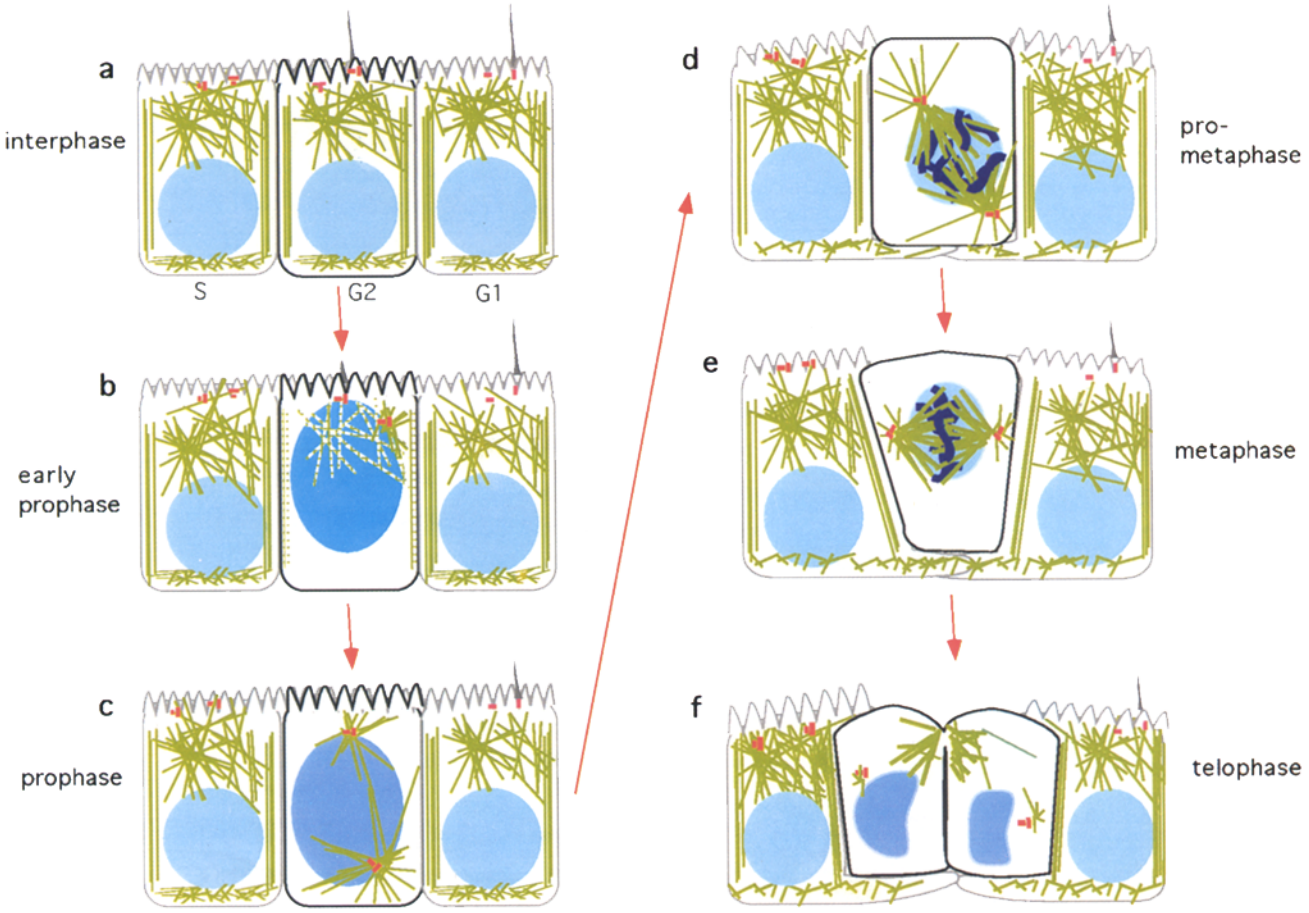

Figure 11. Schematic representation of the changes in the organization of microtubules (*green*), and the localization of centrioles (*red*), or nuclei (*blue*).

ner and Berns, 1976; Roos, 1976; Waters et al., 1993) and the spindle orientation probably occurs once the bipolarity has been established.

Orientation could also occur through the interaction of astral microtubules with specialized cortical sites (for review see Hyman and White, 1987; Strome, 1993). In epithelial cells, the junctional complexes could serve as such sites. It is unlikely that adherens junctions could represent specific positioning sites since they extend over the entire basolateral surface of the cells. Tight junctions are better candidates, but their localization high on the apical surface implies that they would interact with astral microtubules at the top of the spindle, rather than by contacting the poles end-on as in *C. elegans* and *Chaeopterix* (Hyman, 1989; Lutz et al., 1988). This is not necessarily impossible, and if spindle orientation in epithelial cells occurs by this mechanism, the tight junctions remain the best candidates in the absence of other localized structures. Crucial here is the design of experiments to distinguish between spindle orientation due to regional differences in cortical stiffness vs specific spindle attachment sites.

Structural Integrity of the Epithelium during Mitosis

The tight junctions define the borders of the apical and basolateral plasma membrane domains of epithelial cells. Regulation of tight junction assembly and permeability is both rapid and flexible (for review see Gumbiner, 1993). Given the rapid shape changes which occur during mitosis, flexibility in assembly and disassembly of tight junctions is essential if the epithelial seal is to be maintained in the presence of mitotic cells. We have demonstrated here that tight junctions are present during all stages of mitosis (see also Sandig and Kalnins, 1990). The barrier function of epithelia, as measured by the transepithelial resistance, may even increase during mitosis implying that the junctions make even stronger intercellular connections during mitosis than in interphase (Soler et al., 1993). This balance between tight junctions flexibility and strength may be especially important during telophase when the cleavage furrow forms and a tight junction must be assembled between the two new daughter cells. During cytokinesis when the tight junctional complex must increase from a single cell diameter to two cell diameters, it appears that assembly of new tight junctions is not rapid enough to allow expansion of the apical domain along the spindle axis (Figs. 9, *j–l*, 10). Possibly this occurs in G1.

During mitosis protein traffic to and from the plasma membrane as well as between the intracellular membrane compartments is effectively shut down (Souter et al., 1993; for review see Warren, 1993). We observed that two basolateral and one apical plasma membrane protein stay within

the respective membrane domains throughout all stages of mitosis. Thus, the membrane domains are maintained during mitosis and these proteins are not removed from the plasma membrane before mitosis. Previous studies have identified proteins which remain segregated within plasma membrane domains during mitosis in vivo in several epithelial cell types (Tamaki and Yamashina, 1991; Bartles and Hubbard, 1986). The localization of E-cadherin not only gave us information about the maintenance of plasma membrane domains, but also about attachments between the mitotic cell and neighboring interphase cells. During interphase, the adherens junctions are limited to the lateral part of the basolateral membrane. In mitosis, adherens junctions are also present in other locations. In prophase, junctions are present between projections from the surrounding interphase cells which extend both over and beneath the mitotic cell. During cytokinesis, junctions are also found in the cleavage furrow between the two daughter cells. This raises the question of whether E-cadherin is simply redistributed or if insertion into the plasma membrane actually occurs during mitosis. If new protein is inserted during mitosis this is an apparent contradiction to the dogma that protein traffic to the plasma membrane is shut down during mitosis (Warren, 1993). However there are also several reports of some transport which occurs in mitotic cells (Ceriotti and Colman, 1989; Kreiner and Moore, 1990). We also know that mitosis is composed of distinct phases. It is quite possible to have complete inhibition of membrane traffic during metaphase and insertion of new membrane proteins during anaphase and telophase (Souter et al., 1993).

The maintenance of plasma membrane domains during mitosis may allow rapid reassembly of the interphase polarized cytoplasm and therefore minimal interruption of the differentiated function of the epithelial sheet. This also strongly suggests that cell surface polarity is essential to maintain and establish cytoplasmic polarity including microtubule orientation during interphase in epithelial cells (Bacallao et al., 1989; Mogensen and Tucker, 1987; Mogensen et al., 1989; Nakazawa et al., 1992; Tucker et al., 1992).

We are indebted to Ernst Stelzer and Nick Salmon of the EMBL Light Microscope facility for continuous assistance with the confocal microscope, to Tim Stearns and Kai Simons for providing antibodies and to Michael Glotzer and Kai Simons for their thoughtful comments on this manuscript. We would like to thank Rob Parton for providing Fig. 8. The R26.4C monoclonal antibody was obtained from the Developmental Studies Hybridoma Bank maintained by the Department of Pharmacology and Molecular Sciences, Johns Hopkins University School of Medicine, Baltimore, MD, and the Department of Biological Sciences, University of Iowa, Iowa City IA, under contract N01-HD-6-2915 from the National Institute of Child Health and Human Development.

Support for this research was provided by a Human Frontiers Long Term Fellowship to S. Reinsch.

Received for publication 28 March 1994 and in revised form 1 June 1994.

References

Allen, V. W., and D. L. Kropf. 1992. Nuclear rotation and lineage specification in *Pelvetia* embryos. *Development.* 115:873–883.

Bacallao, R., C. Antony, C. Dotti, E. Karsenti, E. H. K. Stelzer, and K. Simons. 1989. The subcellular organization of MDCK cells during the formation of a polarized epithelium. *J. Cell Biol.* 109:2817–2832.

Balcarova-Stander, J., S. E. Pfeiffer, S. D. Fuller, and K. Simons. 1984. Development of cell surface polarity in the epithelial Madin-Darby canine kidney (MDCK) cell line. *EMBO (Eur. Mol. Biol. Organ.) J.* 3:2687–2694.

Bartles, J. R., and A. L. Hubbard. 1986. Preservation of hepatocyte plasma membrane domains during cell division in situ in regenerating rat liver. *Dev. Biol.* 186:286.

Bjerknes, M. 1986. Physical theory of the orientation of astral mitotic spindles. *Science (Wash. DC).* 234:1413–1416.

Brandli, A. W., R. G. Parton, and K. Simons. 1990. Transcytosis in MDCK cells: identification of glycoproteins transported bidirectionally between both plasma membrane domains. *J. Cell Biol.* 111:2909–2921.

Bré, M. H., T. E. Kreis, and E. Karsenti. 1987. Control of microtubule nucleation and stability in Madin-Darby canine kidney cells: the occurrence of non centrosomal, stable detyrosinated microtubules. *J. Cell Biol.* 105:1283–1296.

Buendia, B., G. Draetta, and E. Karsenti. 1992. Regulation of microtubule nucleation activity of centrosomes in *Xenopus* egg extracts: role of cyclin A-associated protein kinase. *J. Cell Biol.* 116:1431–1442.

Buendia, B., M. H. Bré, G. Griffiths, and E. Karsenti. 1990. Cytoskeletal control of centrioles movement during the establishment of polarity in MDCK cells. *J. Cell Biol.* 110:1123–1135.

Ceriotti, A., and A. Colman. 1989. Protein transport from endoplasmic reticulum to the Golgi complex can occur during meiotic metaphase in *Xenopus oocytes. J. Cell Biol.* 109:1439–1444.

Cohen, E., S. Binet, and V. Meininger. 1988. Ciliogenesis and centriole formation in the mouse embryonic nervous system. An ultrastructural analysis. *Biol. Cell.* 62:165–169.

Ferguson, D. J. P. 1988. An ultrastructural study of mitosis and cytokinesis in normal "resting" human breast. *Cell. Tissue Res.* 25:581–587.

Fishkind, D. J., and Y.-L. Wang. 1993. Orientation and three dimensional organization of actin filaments in dividing cultured cells. *J. Cell Biol.* 123:837–848.

Franke, W. W., C. Grund, C. Kuhn, B. W. Jackson, and K. Illmensee. 1982. Formation of cytoskeletal elements during mouse embryogenesis. III. Primary mesenchymal cells and the first appearance of vimentin filaments. *Differentiation.* 23:43–59.

Fujita, S. 1962. Kinetics of cellular proliferation. *Exp. Cell Res.* 28:52–60.

Gelfand, V. I., and A. D. Bershadsky. 1991. Microtubule dynamics: mechanism, regulation and function. *Annu. Rev. Cell Biol.* 7:93–116.

Gumbiner, B. M. 1993. Breaking through the tight junctions barrier. *J. Cell Biol.* 123:1631–1633.

Gumbiner, B., and K. Simons. 1986. A functional assay for proteins involved in establishing an epithelial occluding barrier: identification of an uvomorulin-like polypeptide. *J. Cell Biol.* 102:457–468.

Hyman, A. A. 1989. Centrosome movement in early divisions of *Caenorhabditis elegans*: a cortical site determining centrosome position. *J. Cell Biol.* 109:1185–1193.

Hyman, A. A., and J. G. White. 1987. Determination of cell division axes in the early embryogenesis of *Caenorhabditis elegans. J. Cell Biol.* 105: 2123–2135.

Jinguji, YH., and H. Ishikawa. 1992. Electron microscopic observations on the maintenance of the tight junction during cell division in the epithelium of the mouse small intestine. *Cell Struct. Funct.* 17:27–37.

Joshi, H. C. 1993. γ-tubulin: the hub of cellular microtubule assemblies. *BioEssays.* 15:637–643.

Karsenti, E. 1993. Severing microtubules in mitosis. *Curr. Biol.* 3:208–210.

Kreiner, T., and H.-P. H. Moore. 1990. Membrane traffic between secretory compartments is differentially affected during mitosis. *Cell Regulation.* 1:415–424.

Lamprecht, J. 1990. Symmetric and asymmetric cell division in rat corneal epithelium. *Cell Tissue Kinet.* 23:203–216.

LeBlond, C. P., Y. Clermont, and N. M. Nadler. 1966. The pattern of stem cell renewal in three epithelia (esophagus, intestine and testis). *Seventh Canadian Cancer Conference.* 7:3–30.

Lütcke, H., G. A. Scheele, and H. F. Kern. 1987. Time course and cellular site of mitotic activity in the exocrine pancreas of the rat during sustained hormone stimulation. *Cell Tissue Res.* 247:385–391.

Lutz, D. A., Y. Hamaguchi, and S. Inoue. 1988. Micromanipulation studies of the asymmetric positioning of the maturation spindle in *Chaeopterus* sp. oocytes: I. Anchorage of the spindle to the cortex and migration of a displaced spindle. *Cell Motil. Cytoskeleton.* 11:83–96.

Mack, G., and J. B. Rattner. 1993. Centrosome repositioning immediately following karyokinesis and prior to cytokinesis. *Cell Motil.* 26:239–247.

McNally, F. J., and R. D. Vale. 1993. Identification of katanin, an ATPase that severs and disassembles stable microtubules. *Cell.* 75:419–429.

Mogensen, M. M., and J. B. Tucker. 1987. Evidence for microtubule nucleation at plasma membrane-associated sites in *Drosophila. J. Cell Sci.* 88:95–107.

Mogensen, M. M., J. B. Tucker, and H. Stebbings. 1989. Microtubule polarities indicate that nucleation and capture of microtubules occurs at cell surfaces in *Drosophila. J. Cell Biol.* 108:1445–1452.

Moskalewski, S., and J. Thyberg. 1992. Synchronized shift in localization of the Golgi complex and the microtubule organizing center in the terminal phase of cytokinesis. *J. Submicrosc. Cytol. Pathol.* 24:359–370.

Muresan, V., H. C. Joshi, and J. C. Besharse. 1993. γ-Tubulin in differentiated cell types: localization in the vicinity of basal bodies in retinal photoreceptors and ciliated epithelia. *J. Cell Sci.* 104:1229–1237.

Nakazawa, E., K. Katoh, and H. Ishikawa. 1992. The association of microtu-

bules with the plasmalemma in epidermal tendon cells of the river crab. *Biol. Cell.* 75:111–119.

Oud, J. L., and N. Nanninga. 1992. Cell shape, chromosome orientation and the position of the plane of division in *Vicia faba* root cortex cells. *J. Cell Sci.* 103:847–855.

Palmer, R. E., D. S. Sullivan, T. Huffaker, and D. Koshland. 1992. Role of astral microtubules an actin in spindle orientation and migration in the budding yeast, *Saccharomyces cerevisiae. J. Cell Biol.* 119:583–593.

Parton, R. G., K. Prydz, M. Bomsel, K. Simons, and G. Griffiths. 1989. Meeting of the apical and basolateral endocytic pathways of the Madin-Darby canine kidney cell in late endosomes. *J. Cell Biol.* 109:3259–3272.

Rappaport, R. 1986. Establishment of the mechanism of cytokinesis in animal cells. *Int. Rev. Cytol.* 105:245–281.

Rattner, J. B., and M. W. Berns. 1976. Centriole behavior in early mitosis of rat kangaroo cells (PtK_2). *Chromosoma.* 54:387–395.

Rizzolo, L. J., and H. C. Joshi. 1993. Apical orientation of the microtubule organizing center and associated γ-tubulin during the polarization of the retinal pigment epithelium in vivo. *Dev. Biol.* 157:147–156.

Rodriguez-Boulin, E., and W. J. Nelson. 1989. Morphogenesis of the polarized epithelial cell phenotype. *Science (Wash. DC).* 245:718–725.

Roos, U.-P. 1976. Light and electron microscopy of rat kangaroo cell in mitosis. *Chromosoma.* 54:363–385.

Sandig, M., and V. I. Kalnins. 1990. Reorganization of circumferential microfilament bundles in retinal epithelial cells during mitosis. *Cell Motil. Cytoskeleton.* 17:133–141.

Simons, K., and S. D. Fuller. 1985. Cell surface polarity in epithelia. *Annu. Rev. Cell Biol.* 1:295–340.

Simons, K., and A. Wandinger-Ness. 1990. Polarized sorting in epithelia. *Cell.* 62:207–210.

Smart, I. H. M. 1970*a*. Changes in location and orientation of mitotic figures in mouse oesophageal epithelium during the development of stratification. *J. Anat.* 106:15–21.

Smart, I. H. M. 1970*b*. Variation in the plane of cell cleavage during the process of stratification in the mouse epidermis. *Br. J. Derm.* 82:276–282.

Soler, A. P., K. V. Laughlin, and J. M. Mullin. 1993. Effects of epidermal growth factor versus phorbol ester on kidney epithelial ($LLC\text{-}PK_1$) tight junction permeability and cell division. *Exp. Cell Res.* 207:398–406.

Souter, E., M. Pypaert, and G. Warren. 1993. The Golgi stack reassembles during telophase before arrival of proteins transported from the endoplasmic reticulum. *J. Cell Biol.* 122:533–540.

Stearns, T., L. Evans, and M. Kirschner. 1991. Gamma tubulin is a highly conserved component of the centrosome. *Cell.* 65:825–836.

Stelzer, E. H. K., R. Stricker, R. Pick, C. Storz, and P. Hänninen. 1989. Confocal fluorescence microscopes for biological research. *In* Scanning Imagings. T. Wilson, editor. Proc. Soc. Photo-opt. Instrum. Eng. Bellingham, WA. 1028:146–151.

Strome, S. 1993. Determination of cleavage planes. *Cell.* 72:3–6.

Sulston, J. E., E. Schierenberg, J. G. White, and J. N. Thomson. 1983. The embryonic cell lineage of the nematode *Caenorhabditis elegans. Dev. Biol.* 100:64–119.

Tamaki, H., and S. Yamashina. 1991. Changes in cell polarity during mitosis in rat parotid acinar cells. *J. Histochem. Cytochem.* 39:1077–1087.

Tucker, J. B., C. C. Paton, G. P. Richardson, M. M. Mogensen, and I. J. Russell. 1992. A cell surface-associated centrosomal layer of microtubule-organizing material in the inner pillar cell of the mouse cochlea. *J. Cell Sci.* 1992:215–226.

Vorobjev, I. A., and Y. S. Chentsov. 1982. Centrioles in the cell cycle. I. Epithelial cells. *J. Cell Biol.* 98:938–949.

Warren, G. 1993. Membrane partitioning during cell division. *Annu. Rev. Biochem.* 62:323–348.

Waters, J. C., R. W. Cole, and C. L. Rieder. 1993. The force-producing mechanism for centrosome separation during spindle formation in vertebrates is intrinsic to each aster. *J. Cell Biol.* 122:361–372.

Wright, N., and M. Alison. 1984. The biology of epithelial cell populations, Vol. I. Oxford University Press, Oxford. pp. 56–57 and 211–215.

Zackson, S. L. 1984. Cell lineage, cell-cell interaction, and segment formation in the ectoderm of a glossiphoniid leech embryo. *Dev. Biol.* 104:143–160.

Zeligs, J. D., and S. H. Wollman. 1979. Mitosis in rat thyroid epithelial cell *in vivo* II. Centrioles and pericentriolar material. *J. Ultrastruct. Res.* 66:97–108.